QUANTITATIVE REFLECTION CONTRAST MICROSCOPY OF LIVING CELLS

JÜRGEN BEREITER-HAHN, CECIL H. FOX, and BO THORELL

From the Arbeitsgruppe Kinematische Zellforschung des Fachbereichs Biologie der Johann
Wolfgang Goethe-Universität, Frankfurt am Main, West Germany, the Laboratory of Biochemistry,
National Cancer Institute, National Institutes of Health, Bethesda, Maryland 20014, and the
Karolinska Institutets Patologiska Institution, Karolinska Sjukhuset, Stockholm,Sweden.

ABSTRACT

Mammalian cells in culture (BHK-21, PtK2, Friend, human glia, and glioma cells)
have been observed by reflection contrast microscopy. Images of cells photo-
graphed at two different wavelengths (546 and 436 nm) or at two different angles
of incidence allowed discrimination between reflected light and light that was both
reflected and modulated by interference. Interference is involved when a change
in reflected intensity (relative to glass/medium background reflected intensity)
occurs on changing either the illumination wavelength or the reflection incidence
angle. In cases where interference occurs, refractive indices can be determined at
points where the optical path difference is known, by solving the given interference
equation. Where cells are at least 50 nm distant from the glass substrate, intensities
are also influenced by that distance as well as by the light's angle of incidence and
wavelength. The reflected intensity at the glass/medium interface is used as a
standard in calculating the refractive index of the cortical cytoplasm.

Refractive indices were found to be higher (1.38–1.40) at points of focal contact,
where stress fibers terminate, than in areas of close contact (1.354–1.368). In areas
of the cortical cytoplasm, between focal contacts, not adherent to the glass
substrate, refractive indices between 1.353 and 1.368 were found. This was thought
to result from a microfilamentous network within the cortical cytoplasm.

Intimate attachment of cells to their substrate is assumed to be characterized by
a lack of an intermediate layer of culture medium.

KEY WORDS   quantitative microscopy ·
reflection contrast microscopy · cortical
cytoplasm · interference microscopy · refractive
index

The shape of cells in culture is a result of the subtle
interaction between the macromolecular cytoske-
letal organization (29), the cytoplasmic membrane,
and regions of substrate adhesion. The cytoskele-
ton is composed of structures that maintain tension
as well as flexion (28). Tensile properties are pro-
vided by actin-like filament bundles (22), fine

filamentous networks (27, 31, 13), or intermediate filament loops and bundles (25, 6). Microtubules (7) and, in some special cases, linked actin filaments (brush border, acrosomal process of sperm, reference 30) are examples of structures with the ability to exert or to withstand pressure (25).

Most animal cells are attached to a surface (i.e., other cells, basal lamellae, collagen). Here, shape is basically determined by the action of contractile and tensile elements in concert with zones of adhesion. The insensitivity of cell spreading to colchicine (15, 14) exemplifies the secondary role of microtubules in maintaining the shape of isodiametric cells. The formation of asymmetric processes, on the other hand, as in spindle-shaped fibroblasts or neuronal cells and their melanocyte derivatives (8), depends on ordered microtubular arrangements. Any explanation of cell shape or its changes during movement must therefore be based on the interaction between filaments, microtubules, adhesive zones, and the limiting membrane. While the arrangements of filaments and microtubules have been studied by electron microscopy (33, 13) and by immunofluorescence techniques (20, 32, 25), electron microscopy has been thought to be of limited value for investigation of cell substrate attachment due to fixation or dehydration artefacts (29).

Several attempts have been made to visualize the underside of cells and their attachment to surfaces at the light microscope level. Ambrose and Jones (3) used a reflection microscope arrangement with very oblique illumination to demonstrate attachment sites of cells to glass. Ingram (18) reported that side views of cells were not suitable for the study of cellular adhesion to glass.

Curtis (9) invented an interference reflection contrast microscope, based on low-angle, vertical illumination of the specimen through the objective lens by a high-intensity mercury arc lamp. Only a small amount of this light is reflected. The reflected light, as densities produced on photographs, was measured by a Joyce-Loebl microdensitometer. From these densities, Curtis was able to calculate the distances of the cells from the coverglass at specific regions. The method was improved by Izzard and Lochner (19, 21), mainly by increasing the numerical aperture of the illuminating system. This system has also been used by Abercrombie and Dunn (1) for the study of adhesion of fibroblasts to a substrate during contact inhibition, as well as by Heath and Dunn (17) and

Dvorak (10). Ploem (26) introduced oblique illumination by using a ring-shaped illuminating aperture and a combination of linear and circular polarized light to exclude stray light.

We have studied the attachment of several types of cells to glass with an improved Leitz-Ploem apparatus in combination with electron microscopy. In this paper, we present a theoretical evaluation of reflection contrast microscopy, and demonstrate its use with appropriate cellular systems.

MATERIALS AND METHODS

Cells and Cell Culture

(a) BHK-21 cells, a fibroblast-type line obtained from the Bundesanstalt f. Viruskrankheiten der Tiere, Tübingen (kindly provided by Prof. Dr. W. Schwöbel). The cells were grown in PM 13 medium (Serva, Heidelberg). (b) Human glia cells and human glioma cells (obtained from the Karolinska Institutet, Stockholm, kindly provided by Dr. P. Collins) grown in NCTC 199 (glucose-free) medium supplemented with 10% dialysed calf serum and 10 mM glucose. (c) PtK 2 cells (kindly provided by Dr. Osborn, Max Planck Institut f. Biophysikalische Chemie, Göttingen) grown in McCoy's 5A medium (Grand Island Biological Co., Grand Island, N. Y.). (d) Friend cells (12) were grown in MEM Alpha medium supplemented with 10% fetal calf serum and antibiotics (penicillin, streptomycin, fungizone), at a concentration of ~3 × 10^5 cells/ml (kindly provided by Dr. R. Zucker, Papanicolaou Cancer Res. Inst., Miami, Fla.).

For microscope observations, all cells except Friend cells were grown on coverslips, mounted either in Rose chambers, in Dvorak-Stotler chambers (Zeiss, Oberkochen), or in a chamber described by Ploem (26). Friend cells, however, were allowed to settle on polylysine-coated coverslips for 1 h before observation.

Photographic Methods

Photographs were taken with Combiphot II equipment (Leitz, Wetzlar) either on Ilford FP4, 35-mm negative film or on Kodak Tri-X negative film and developed in Microphen or Microdol, respectively. Densities of the negatives were recorded with a Joyce-Loebl microdensitometer (×10 objective lens, ×20 Searle enlargement). Zero was set with the unexposed parts of the film between frames. Cell-free areas represented the reference level of intensities calculated from Eq. 1 (see below). Measurements of negatives taken of the same image, but with different exposure times, have been used to insure that all grey levels under normal exposure times were in the linear density range.

Electron Microscopy

For electron microscopy, BHK-21 cells were fixed in

3% glutaraldehyde (in 0.1 M phosphate buffer, pH 7.2) at room temperature, postfixed in 1% phosphate buffered OsO_4, dehydrated in ethanol and embedded in Epon-Araldite. Cells were removed from the glass substrate by plunging into liquid nitrogen and re-embedded in Epon-Araldite. The Friend cells were fixed the same way but embedded in Araldite. These preparations were provided by Dr. M. Cayer (Papanicolaou Cancer Res. Inst.).

Instrument Design

The reflection contrast microscope used for these studies consists of a Diavert inverted research microscope (Leitz, Wetzlar) supplemented by a 200-W mercury arc illuminator, a polarizer, and a second collimating lens in the incident illuminator stand. The HBO 200 lamp allows better illumination of the ring-shaped illuminating aperture (Fig. 1, i.A.) than the more efficient HBO 100 supplied by the manufacturer. The image of the source annulus (illuminating aperture) coincides with the phase ring at the rear aperture plane of the objective. The objective optical system consists of a Ploempak '2.2' equipped with a semireflecting plate and an analyzer. Two phase objective lenses are available with ¼ wave plates attached to their front elements with the slow axis
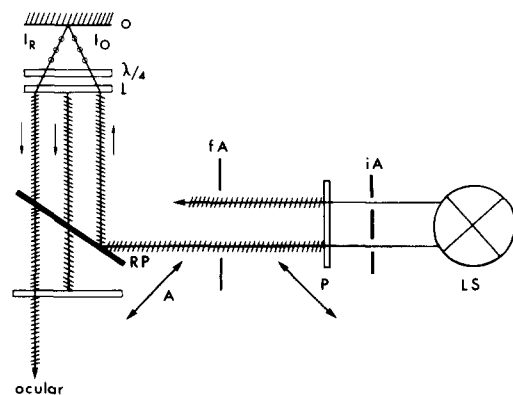

FIGURE 1 Diagram of the Leitz-Ploem reflection contrast system. Light from a mercury arc lamp (LS) penetrates a ring shaped illuminating aperture (iA), and is linearly polarized by a polarizer (P). The field limiting aperture (fA) is focused in the object plane. A semireflecting plate (RP) directs the beam to the objective lens (L) without any change in polarisation. The light is projected on the object (O), where it has the intensity I_o. A quarter wave plate ($\lambda/4$) causes circular polarisation of the illuminating beam and linear polarisation of the reflected beam (I_R), but with a 90° difference in the direction of polarisation. Therefore, I_R penetrates the analyzer (A) crossed to the polarizer. Light reflected from the lens surfaces (beam exemplified between the main paths) with unaltered polarisation does not cross the analyzer. To simplify the diagram, only one part of the light beam penetrating i.A. is followed.

at 45° to the polarizer's direction (Fig. 1): an oil immersion ×100 NA 1.30 and a ×40 1.00. The dark central part of the ring-shaped i.A. exceeds the outer diameter of the phase ring. Therefore, the phase ring does not appreciably influence the reflection contrast image. The combined phase-reflection optics allow an easy comparison of either phase or reflection contrast images of a cell simply by changing illuminating systems.

The illuminating aperture gratings provided by the manufacturer give limited possibilities for the increased illuminating apertures that are essential for eliminating lower order interference. For this purpose, a new aperture ring was constructed that consisted of a central circle 8 mm wide and an outer ring of 10 mm. In connection with the ×100 objective lens, this allows the use of an incidence angle of 34.9°–45.9°, which represents a considerable increase over the 11.8°–30.1° aperture provided by the manufacturer. The higher illuminating aperture allows improved quantitative estimations of cell attachment.

Interpreting the Reflection Contrast Image

Interpretation of images generated by reflection contrast microscopes is enhanced and simplified if one differentiates between simple reflected light and interference produced by reflected light.

PARTICIPATION OF REFLECTION AND INTERFERENCE IN IMAGE FORMATION: In a system where cells are growing on a glass surface, only four interfaces are of major importance as a source of reflection (Fig. 2) when oil immersion objectives are used. These are: (a) glass/cell (gc), (b) glass/culture medium (gm), (c) culture medium/cell's lower surface (mc), (d) cell's upper surface/culture medium (cm).

The relative intensity (R) of the reflected light (I_r) at an interface between two media as a function of the incident light (I_o) is obtained from the refractive indices n_1 and n_0 as in:

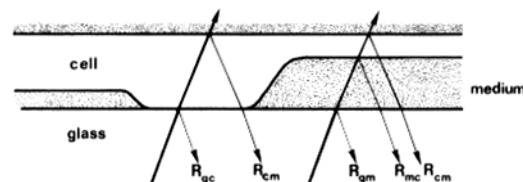$$R = \frac{I_r}{I_o} = \left[\frac{n_1 - n_0}{n_1 + n_0}\right]^2 \qquad (1)$$

FIGURE 2 Schematic representation of the main reflecting interfaces in a cell preparation on a coverglass. The thick arrows indicate the incident beams, the thin arrows, the reflected beams with the relative intensity R. The suffixes indicate the optical media forming the interface. The phase of R_{mc} is shifted for $\lambda/2$ at the reflecting surface.

If the following refractive indices for the three optically different phases in cultures are: glass, $n_g = 1.5150$, culture medium $n_m = 1.3371$, and cells $n_c = 1.370$ (30), then the greatest difference in the refractive indices occurs at the glass/medium interface.

The relative values for the reflectivity of the different interfaces can be calculated according to Eq. 1, demonstrating that cell-free areas (glass/medium interfaces) represent the brightest zones. Thus, light intensities in a reflection contrast microscope image which are higher than the intensity at the glass/medium interface, i.e., brighter, must be due to interference, while lower intensities, i.e., darker areas, can be either due to interference or to increased reflectivity at the glass/cell interface. In an image composed of reflected rays modulated in intensity by interference with each other, the cell-free areas can be used as a reference for the calculation of intensities in other regions of the preparation provided, as here, the use of circularly polarized light has avoided the problem of polarization-dependent reflection.

CALCULATION OF THE REFRACTIVE INDEX OF THE CORTICAL CYTOPLASM BY MEASUREMENT OF ITS REFLECTIVITY: To use reflectivity for calculations, all reflected light must be gathered by the objective lens.

In the Leitz-Ploem system the illuminating beam is limited by a ring-shaped aperture similar to that used for phase contrast illumination, coincident with the back plane of the objective. When a specimen is uniformly illuminated by oblique rays emanating from the front surface of the objective, all light reflected from a perpendicular surface will be collected by the lens. When the surface is not perpendicular to the optical axis, the reflected light will be recovered only if the illuminating angle is smaller than the angular aperture of the objective.

$$N_c = N_g \left[\frac{1 + r_{gc}}{1 - r_{gc}} \right] = N_g \left[\frac{1 \pm \sqrt{R_{gc}}}{1 \mp \sqrt{R_{gc}}} \right]. \quad (2)$$

Eq. 2 is derived from Eq. 1 for reflectivity (R), where R_{gc} is the reflection intensity (a positive or negative value depending on the relation between the two refractive indices) and r_{gc} the amplitude reflectance coefficient. Figs. 6 and 9 illustrate the determination of R_{gc} by densitometry of a photographic image. Film density over background in cell-free ares of the preparation is set for 0.398% (reflection at the glass/medium interface, from Eq. 1, where $n_m = 1.3371$, so that $R_{gm} = 0.398\%$ of I_o).

EVALUATION OF INTERFERENCE PHENOMENA: When a cell attached to a coverglass is observed, rays reflected from the medium/cell or cell/medium interface can interfere with rays reflected from the glass/medium interface. The highest of these reflection intensities, as already stated, occurs at the glass/medium interface. Consequently, brightness levels higher than those at this interface can only be produced by interference. On the

other hand, darker areas may be caused either by partial extinction due to interference or to a diminished reflectivity where a cell is in contact with the coverglass. The intensity (I) of a composite beam resulting from interference of two beams reflected at different interfaces (glass/medium or medium/cell) can be calculated by the expression:

$$J = \left(\frac{n_g - n_m}{n_g + n_m} \pm \frac{n_c - n_m}{n_c + n_m} \times \cos \frac{4\pi n_m \cdot d \cos \beta}{\lambda} \right)^2$$
$$+ \left(\frac{n_c - n_m}{n_c + n_m} \times \sin \frac{4\pi n_m \cdot d \cos \beta}{\lambda} \right)^2 \quad (3)$$

which is derived from the calculations resulting from the interference of two parallel coherent beams (23). In this formula:

$$\frac{4\pi \cdot n_m d \cos \beta}{\lambda}$$

= path difference between the interfering beams.

β = the angle of incidence at the reflecting surface. $\pm$ = $(-)$ phase shift of $\lambda/2$ for the reflection from optically denser medium, i.e., at a medium/cell interface, $(+)$ interface with reflecting medium of lower refractive index, i.e., the glass/medium interface. d = distance between glass and cell surface filled with culture medium with the refractive index n_m.

To use this formula (Eq. 3) for quantitative measurements, the angle β, the wavelength of the monochromatic illumination and the refractive index of the reflecting cell surface must be known.

The refractive index of cortical cytoplasm not in contact with the substrate can be estimated according to Eq. 2. Areas that appear bright on photographic prints (Figs. 8b and 9) are due to the summation (interference) of rays reflected at the glass/medium interface and the medium/cell interface.

An optical path difference of $\Gamma = \lambda$ between the interfering beams is assumed to facilitate calculation: The intensity resulting from the interference of two coherent beams with a phase difference of λ equals $(\sqrt{R_{gm}} \pm \sqrt{R_{mc}})^2$. R_{mc} is used in Eq. 2 for the calculation of the refractive index of the cell at the medium/cell interface. Coherence can be assumed for small lateral distances between the interfering beams r_{gm} and r_{mc} and small optical path differences (1 to 2λ).

In the Leitz-Ploem system, the angle of illumination (α) ranges between 10.6° and 30.5° with the ×40 objective and from 11.8° to 30.1° with the ×100 lens. This range is determined by the width of the ring-shaped aperture in the illuminating aperture. With the commercially equipped system, considering the refraction law, the real angle of incidence at a medium/cell interface (β) perpendicular to the optical axis ranges from 12.1° to 35.2° for the ×40 and from 13.4° to 34.8° for the

×100 lens. The differences in cos β (0.98/0.82 and 0.97/0.82) influence the phase differences between the interfering rays and cause a loss in contrast of higher order interference fringes. The imprecise definition of β makes an exact determination of d (distance between glass and cell surface) impossible. Nevertheless, this distance can be estimated from the optical path difference at $\lambda/2$ intervals with sufficient accuracy for most biological purposes by:

$$d = \frac{(\Gamma - \lambda/2)}{2n_m \cdot \cos \beta},\tag{4}$$

where $\lambda/2$ represents the phase shift at the medium/cell interface.

Calculations of cell/glass distance based on the intensity of a beam resulting from the interference of rays reflected by the glass/medium and the medium/cell interfaces (9) are restricted to cells of known cortical cytoplasm refractive index. The uncertainty of this value prohibits any accurate calculation of cell/glass distance based on intensity measurements at a single wavelength. Evaluation is only possible in steps of $\lambda/2$, where the phase difference can be directly recorded (Eq. 4), or with a two wavelength system.

DISCRIMINATION BETWEEN REFLECTION AND INTERFERENCE: Reflection and interference phenomena may be separated from each other by varying the optical conditions of the system. The two simplest methods consist of using either a two-wavelength method or different illuminating apertures. In the first case, the intensity of resulting interference is altered due to differ-
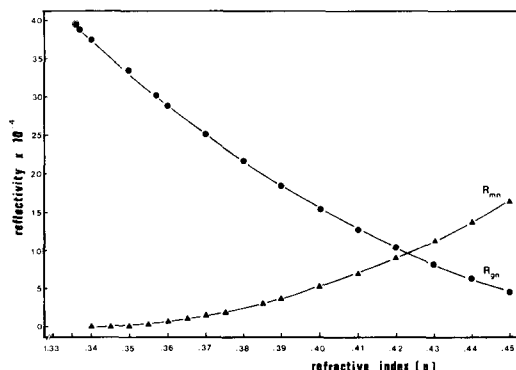

FIGURE 3 Relation between the refractive index (n) of the nonabsorbing specimen and the relative intensity of reflected light (reflectivity) at the interface to glass (n_g = 1.515, R_{gn}) and medium (n = 1.3371, R_{mn}). The circled dot (upper left corner) indicates the reflectivity at the glass/medium interface. R_{gn} can be used to determine the refractive index of cellular regions, which are in intimate contact with the glass. R_{mn} is the intensity available for the modulation of R_{gm} (circled dot) by interference.

ences in the apparent optical path length. Fig. 4 shows the effect of photographing cells in green (546 nm) and blue (436 nm) light. All regions of the cell which are not in direct contact with the glass exhibit an altered intensity, whereas contact zones remain unchanged. To a first approximation the intensity of reflection is independent of the wavelength of the illuminating beam, so that interference phenomena are altered by the change in wavelength while the intensity of reflection is not. Optical dispersion causes a change of refractive index of culture medium in the range of 0.0001–0.0004 between wavelengths of 546 nm and 436 nm. The dispersion of the glass is also negligible because the determination of glass/cell reflectivity is always related to the glass/medium reflectivity. The optical dispersion of the cell is unknown but can be estimated to be in the same range as a serum-containing medium.

Fig. 5 shows the results of employing the second method of visualizing cell-substrate attachment, i.e., altering the illuminating aperture. As with the two-wavelength method, points of direct contact are clearly delineated while interference causes other parts of the cell to disappear or appear with altered intensities. Higher order interferences caused by the cell/medium interface also disappear.

The use of optical variables (e.g., different wavelengths or illuminating apertures) is a valuable method for determining the attachment points of cells to a glass substrate. The two-wavelength method used here allows one to determine which areas are in direct contact, using reflection, and which areas are not in direct contact, using interference. Further, observations of direct contact made with the two-wavelength method may be readily confirmed by changing the illuminating aperture and vice versa. While optical methods cannot determine whether cells are attached to the glass via an intermediate pad of glycoprotein (29), the intimacy of the attachment points as determined by the two-wavelength method is clear, and is characterized by the absence of culture medium between the glass surface (or protein film) and the cell.

APPROXIMATION OF THE LIMITS OF THE REFLECTION INTERFERENCE SYSTEM USED: First, the degree of background intensity modulation necessary for a clear intensity determination by densitometry of a film negative was estimated to be 10%. This is due to the modulation of R_{gm} by R_{mc}. For the purpose of approximation, a maximal value of 1.45 for the refractive index of the cytoplasm adjoining the attachment points was chosen (cortical cytoplasm). If light at a wavelength of 546 nm with vertical ($\beta = 0°$) illumination was used, this minimal 10% modulation would occur for a glass/cell distance of 0.12 λ or 65 nm (calculated from Eq. 1). If the illumination was at an angle of 30°, a distance of 52 nm could be detected. For a refractive index of 1.40, the values were altered to 200 nm at 546 nm with 30° illumination. With a shift to a lower wavelength (436
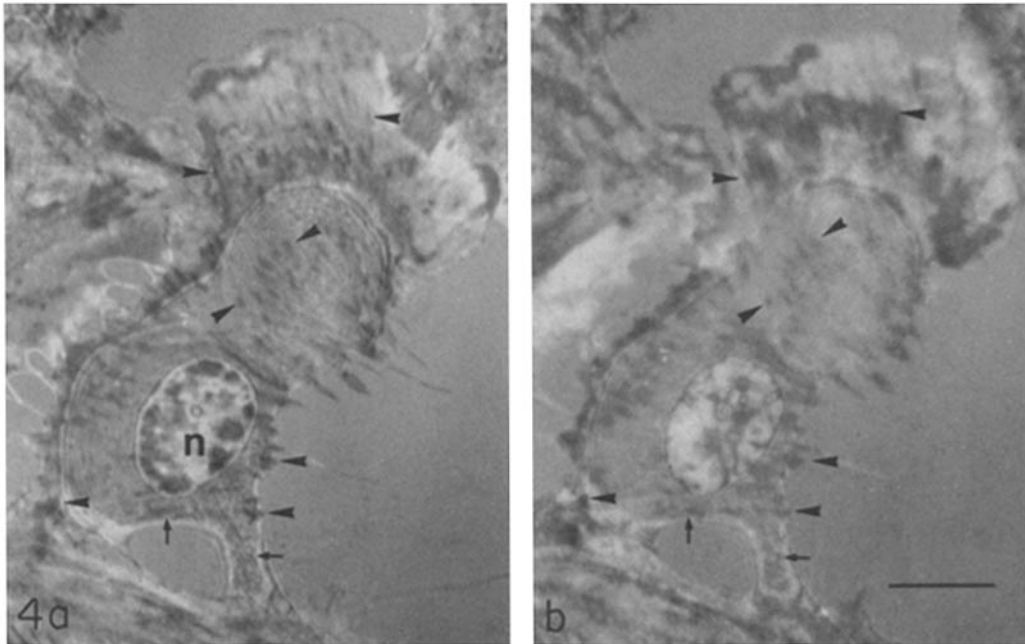
FIGURE 4   Influence of the wavelength on the reflection contrast microscope image of a PtK 2 cell. Illumination conditions: (a) monochromatic light, 546 nm, (b) blue light, mainly of 436 nm: BG 12, BG 38, HBO 200 mercury lamp. Distinct differences occur predominantly in the lamellipodia (upper part of the central cell and lower right region of the cell at the left margin) and the nucleus (n). The darker spots (arrowheads) and the broad medium grey zone (arrow) remain nearly unchanged. Bar, 10 μm.

nm), a separation of 160 nm was detectable with a cellular refractive index of 1.40 and 30° illumination. While the relationship between absolute values for refractive index and reflectivity is shown in Fig. 3, these may depend on the angle of illumination. The values used here are based on comparative estimations of R_{gc} (or R_{mc}) from R_{gm} and thus differ less than the absolute values. Measurements at angles in excess of 35° were not used for quantitative calculations.

RESULTS

Calculations based on reflection contrast densitograms according to Eq. 2 show that there are three different regions of optical density produced by the cytoplasm lying over the supporting substrate: (a) Regions closely attached to the substrate but without special differentiations (close contacts) show a refractive index between 1.354 and 1.368 (in BHK-21 cells, Fig. 6). These values correspond to a relative dry mass of between 12% and 20% (calculated on the basis of a specific refractive increment = 0.0018, [16, 11, 24, 31]). (b) In focal contacts (Figs. 6 and 7), where stress fibers terminate (17), the refractive index ranges from 1.38 to 1.40, which is equivalent to relative dry mass concentrations of 27% to 38%. (c) Regions of the cell between focal contacts and not in direct contact with the substrate exhibit refractive indices from 1.353 to 1.368 (Figs. 8 and 9), corresponding to 11% to 19% relative dry mass concentration.

Electron micrographs of attached BHK-21 cells cut vertically confirm the light microscope findings, that is, portions of the cell directly above focal contacts (Fig. 10) show a considerable increase in the apparent density of the cytoplasm corresponding roughly to the increase in refractive index detected by light microscopy.

Where close contacts are found in electron micrographs, the cytoplasm is less dense (Fig. 11) due in part to a decrease in the amounts of fibrillar structures but also to a decrease in the amounts of dense amorphous cytoplasmic substance.

In portions of the cortical cytoplasm between focal contacts, where there is no intimate contact with the substrate, the cytoplasm is characterized by a fine filamentous material (Fig. 12). The high variability of refractive indices in this region and in zones of close contact is probably due to differ-
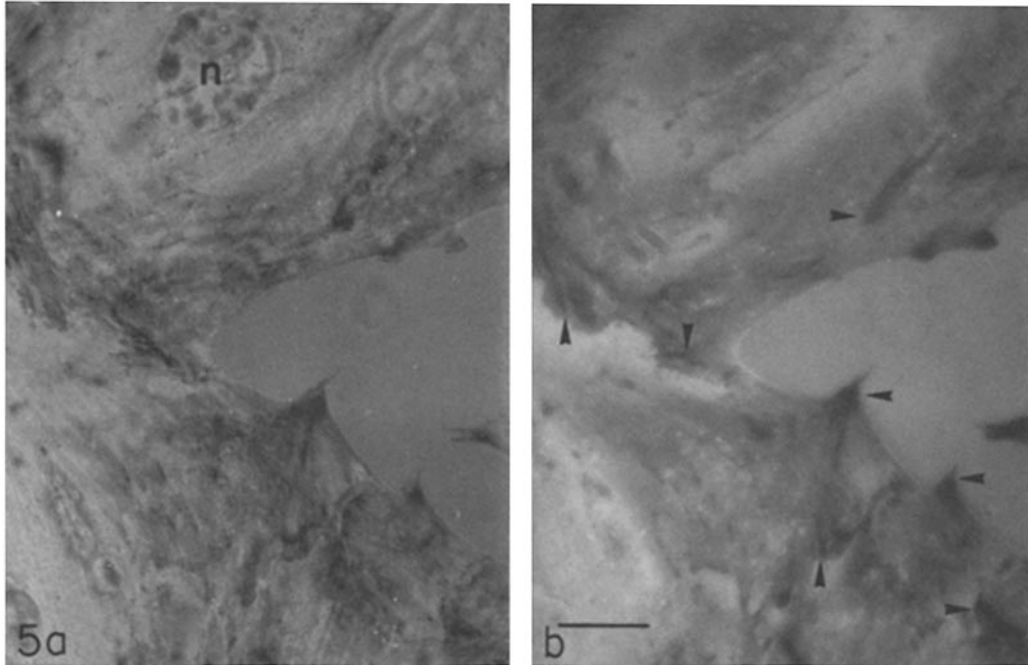
FIGURE 5 Influence of the illuminating aperture (iA) on the appearance of PtK 2 cells in the reflection contrast microscope. (*a*) 0.31–0.76 iA, objective ×100; (*b*) same objective lens, 0.87–1.09 iA. The nucleus (*n*) has nearly disappeared; only points of attachment appear black (arrowheads); the spatial relations of adjacent cells are clearly defined (dark: close to the glass, bright: nonadhering zones with greater distance to the glass); the focal depth is smaller, therefore less influence of deeper cytoplasmic regions and fewer regions in focus. Bar, 10 μm.
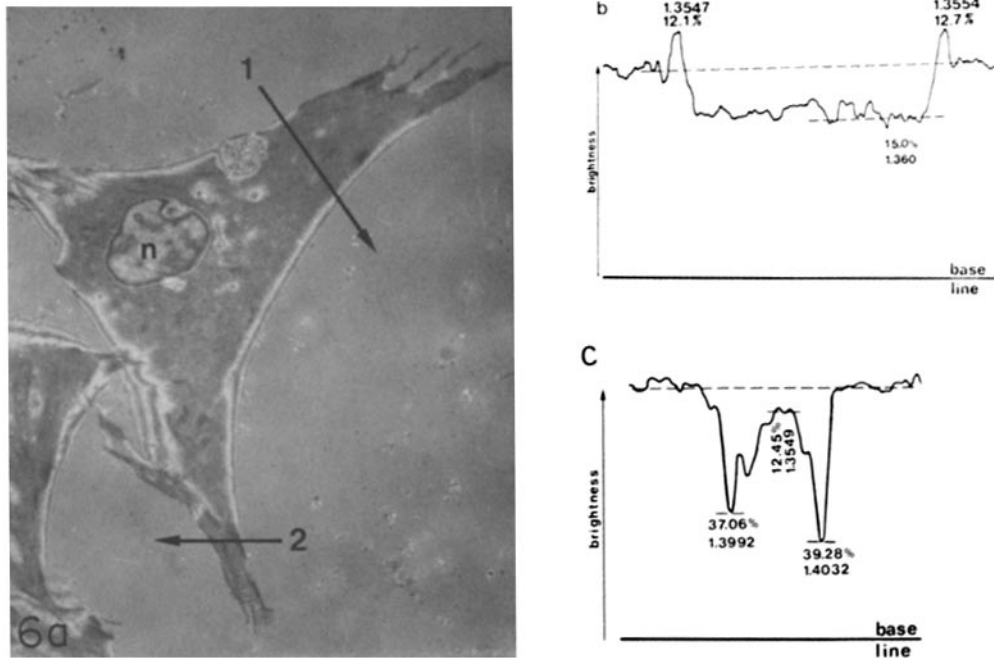
FIGURE 6 (*a*) BHK-21 cell in reflection contrast, objective ×100. A broad grey area indicates the region of smooth, intimate contact to the glass. Rod-shaped focal contacts occur in the periphery of the cell. The nucleus (*n*) is visible. At bright margins or spots the cytoplasm does not touch the coverglass. Arrows indicate the scanning line for the densitograms. (*b* and *c*) Densitograms through the negative of *a*. *b* at position 1, *c* at position 2. For further explanation see text.
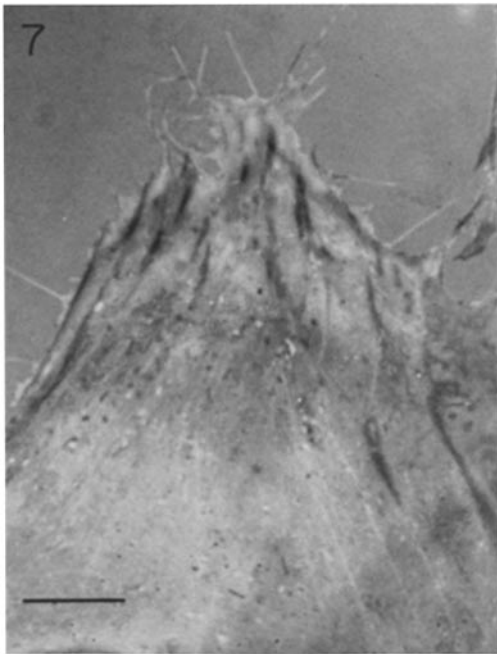
773

FIGURE 7 Reflection contrast microscope image of a human glia cell (objective ×100). Fibrils (stress fibers) are running into the dark attachment plaques (focal contacts) at the cell margin. Thread-like processes are straight forward protruding from the cell. The are common in most tissue culture cells (see also Fig. 8), and can hardly be detected by phase contrast microscopy. Nothing is known about their function. Bar, 10 μm.

ences in the density of this cortical filament layer.

In Friend erythroleukemia cells and motile lymphocytes there is no formation of focal contacts (Fig. 9). The central part of the Friend cells' cytoplasm adherent to polylysine-coated coverglasses was determined to have a refractive index of 1.3632 (17% relative dry mass). The marginal cytoplasmic border of these cells, which is composed exclusively of a fine filamentous network (Fig. 13), has a refractive index of 1.38 (28–29% relative dry mass). While this filamentous network is confluent with a cortical network where the cell is in contact with the medium, no such filamentous layer is seen where the central cytoplasm is attached to the glass (Fig. 13). Instead, both Friend cells and motile lymphocytes appear to attach via close contacts, especially when cultivated on polylysine-coated surfaces.

The fibroblastoid BHK-21 cells and PtK2 cells, however, exhibited small elongated attachment zones (focal contacts, reference 19) as well as broad

adhesion zones (close contacts, reference 19). Fibrillar arrays (stress fibers) terminate in the focal contacts (Fig. 7) as was demonstrated by Heath and Dunn (17). Focal contacts were also found in human glia cells and in the glioma cell line (Fig. 8).

BHK-21 cells prepared for electron microscopy and cut in cross-section show a broad range of cell to substrate separations. In addition, the surface of the substrate appears to be covered by a film that may represent the protein film proposed by Revel and Wolken (29). The distance between the cell membrane and this film ranges from intimate contact (<20 nm) at points of focal contact up to one or more microns. The most common separations were those around 70 nm ± 10 and between 150 and 200 nm. However, it should be pointed out that shrinkage artefacts caused by fixation, dehydration and embedding for electron microscopy are not rigidly controllable.

DISCUSSION

While our studies using reflection contrast images differ in approach from those previously reported by Curtis (9) and Izzard and Lochnar (19), they both support and extend these valuable contributions. The principal difference lies in the interpretation of the nature of the direct contacts between cell and glass. While our optical methods cannot determine whether cells are attached to the glass via an intermediate pad of glycoprotein (29), the intimacy of the attachment points as determined by the two-wavelength method is clear, and may be characterized as the absence of culture medium between the glass surface (or protein film) and the cell. Indeed, lack of a medium layer at sites of direct contact may explain why Izzard and Lochner (19) were unable to detect alterations in the brightness of dark attachment zones after changing the refractive index of the culture medium. These areas of direct contact with the supporting glass surface provide an opportunity for accurate and simple determinations of their refractive index.

The actinomyosin nature of cortical filaments in cultured mammalian cells is well established (13, 33, 27). Cellular regions in contact with the substrate have a lower refractive index at broad regions of attachment (close contacts) than at focal contacts. Further, measurements reveal refractive indices (corresponding to 11–19% dry mass) for non-attached regions of the cortical cytoplasm in BHK-21, human glioma, and Friend cells, which
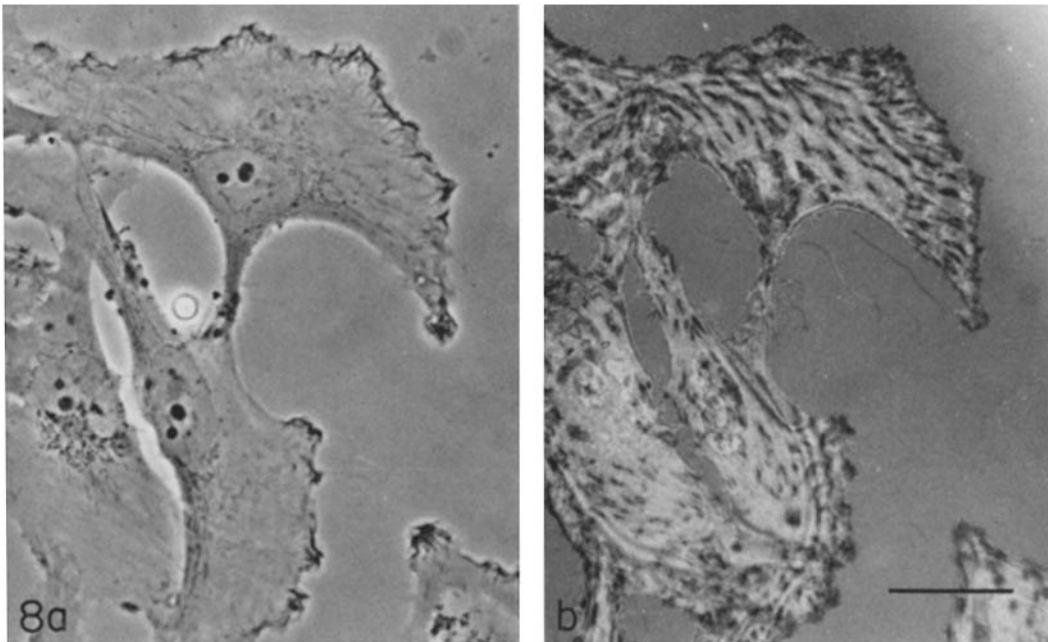
FIGURE 8 Human glioma cells; (a) phase contrast. (b) reflection contrast. In b, attachment plaques are clearly visible, while the ruffling (on the medium side of the cell) is only seen in phase contrast (a). Bar, 100 μm.
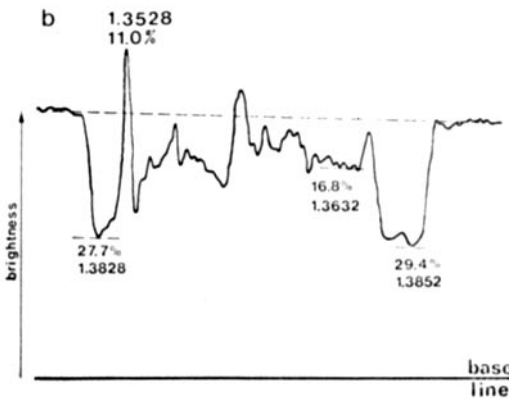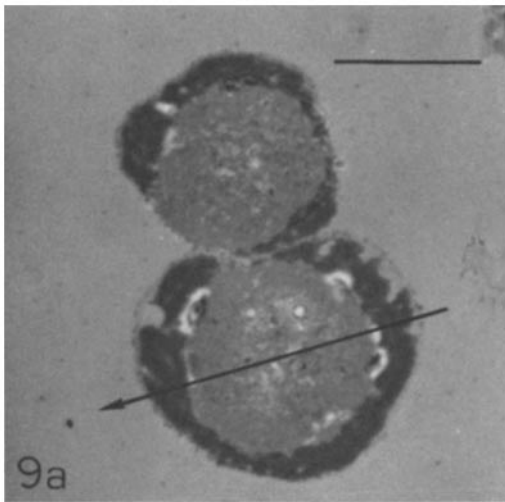
FIGURE 9 (a) Erythroleukaemic cells (Friend cells) in reflection contrast. The central cytoplasm is surrounded by a dark marginal cytoplasmic border, which is detached from the supporting glass at the bright areas. Most of the central cytoplasm appears homogeneously grey. (b) Densitogram through the cell of a, as indicated by the arrow line. Bar, 10 μm.

correspond to those of close contacts.

These observations may be summarized as follows: (a) Broad close contact areas with low refractive index either lack a cortical filamentous network (as in the central areas of Friend cells) or have such a network in a relaxed state. (b) Focal contacts anchor stress fibers to the substrate (17). Protein as well as some dense substance at the point of attachment are responsible for a relatively higher refractive index (1.38–1.40) than is seen in close contacts. (c) The large range of values obtained for the cortical cytoplasm in areas between focal contacts and in the close contacts may be

influenced by the organization and the contraction of the filamentous network. Such a contraction could cause tension between the attachment points (28).

Rees et al. (28) have discussed the importance of cellular stiffness for attachment. This stiffness is probably due, at least in part, to contraction of the cortical filamentous network of the cells. Beck et al. (4), in support of these observations, found that the amount of protein per unit area in threads of randomly organized and purified actinomyosin increased 18-fold after contraction.

The reflective properties of a cell at a glass/cell interface or a cell/medium interface may be due to (a) reflection from the plasma membrane and the adherent glycocalyx, (b) reflection from the cortical cytoplasm, or (c) the cytoplasm being physically homogeneous.

Since a phospholipid double layer at an air/water interface acts as a reflecting medium, the first of the above possibilities seems the most likely. The plasma membrane does not apparently form a second interface with the cytoplasm, perhaps because there is an intimate connection between membrane proteins and the cortical filamentous network. Thus, the optical properties of the cell at an interface depend on the complex formed by both the cytoplasmic membrane and the cytoplasmic components closely associated with the membrane, rather than on the membrane alone.

Incident illumination results in equal light intensities throughout the focal space. The depth of this space depends on the angle of illumination and determines the upper limit of the material involved in reflection. For the NA 1.3 ×100 lens used with a high angular aperture of illumination, this is ~500 nm. The thickness of the filamentous network does not exceed 200 nm and it can be assumed to have a higher refractive index than the underlying cytoplasm. It is therefore this network that defines the reflective properties of the upper cell surface.

It seems clear from our observations and those of others that there is a clear connection between the various types of attachment sites and the mechanisms by which cells attach to a substrate. These attachment sites represent areas of specialization of the cortical cytoplasm and cell membrane that are involved not only in attachment but the dynamic functions associated with cell movement over a supporting surface.

The reflection contrast microscope provides a
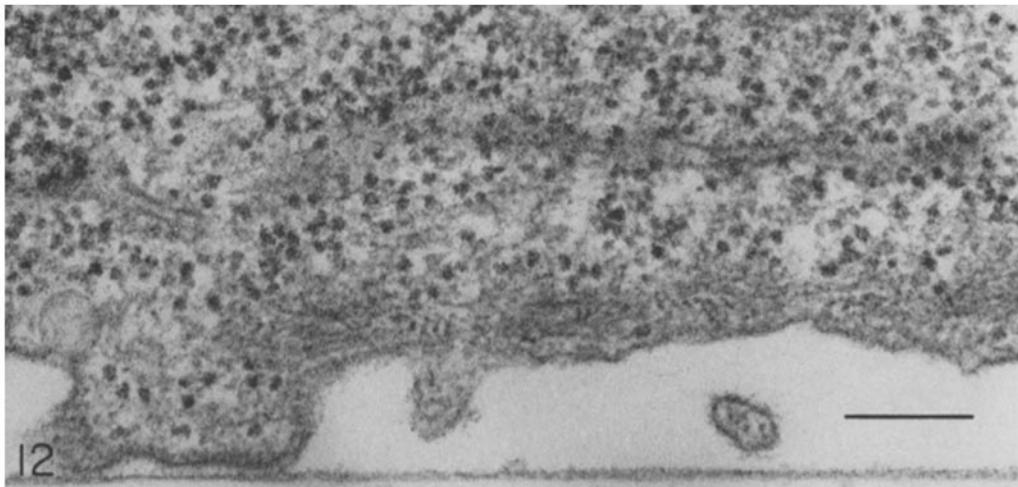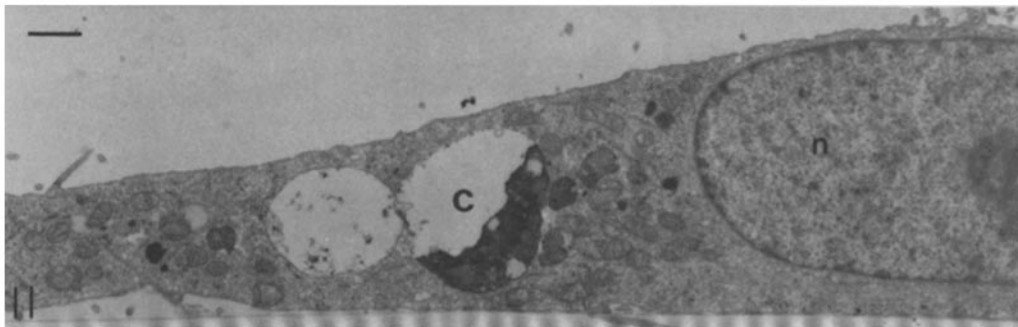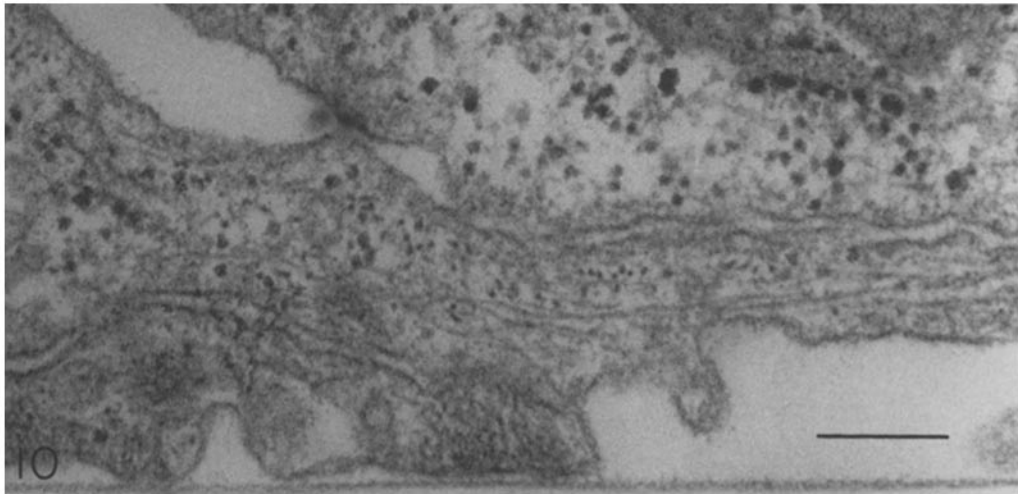
Figures 10, 11, and 12   Electron micrographs of cross-sectioned BHK-21 cells growing in a fibroblast-like manner. The line parallel to the lower margin represents probably a protein film on the coverslip.

Figure 10   Filament bundles in the right half of focal contact. It is obvious to assume a high difference in the refractive index between the right and the left part of this plaque. Bar, 0.2 μm.

Figure 11   The central part under the nucleus (n), is closely apposed to the substratum (close contact), while the periphery is more or less apart. (c) vacuolic cytosome. Bar, 1 μm.

Figure 12   The attachment zone is nearly free of filamentous material, while the cortical cytoplasm of the nonadhering region is composed of a filamentous material. Bar, 0.2 μm.
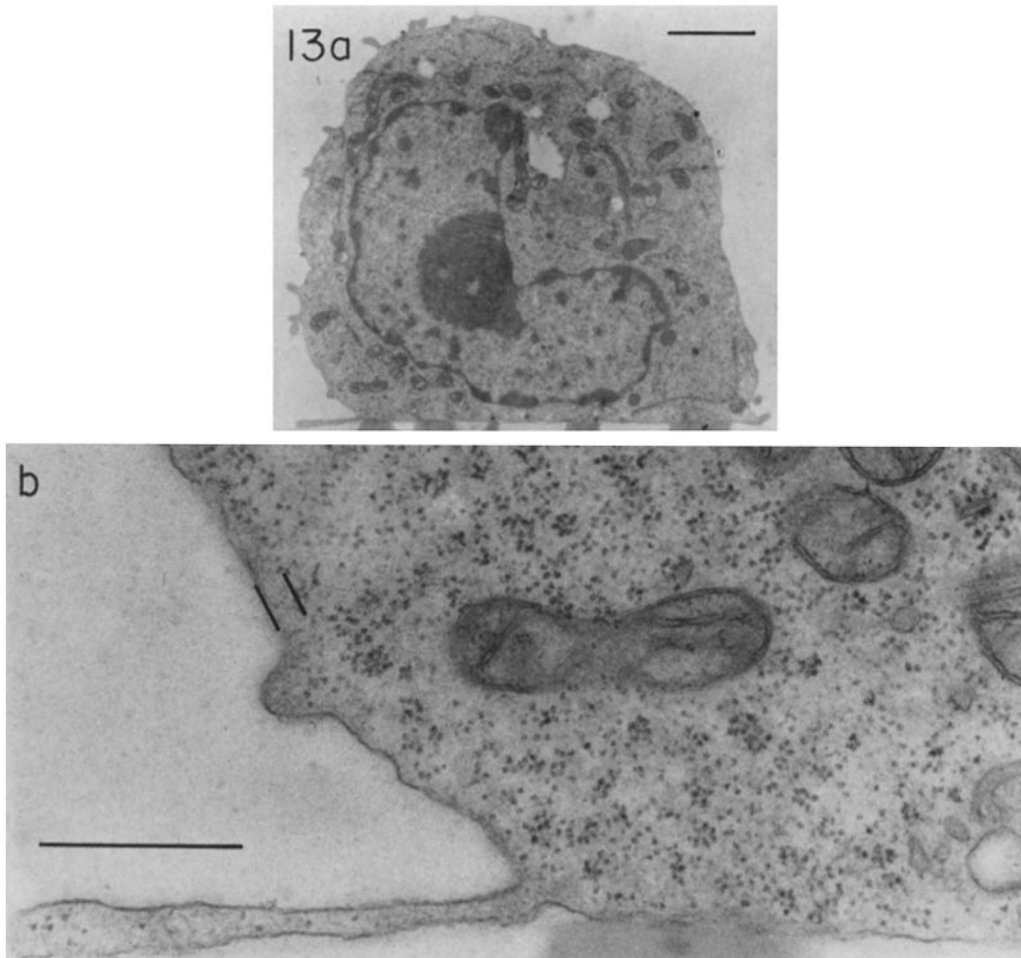
FIGURE 13 Electron micrographs of cross-sections of Friend cells, settled on a polylysine-covered petri dish. The more or less spherical cell is smoothly attached to the substratum. The very delicate marginal cytoplasmic layer is clearly identified. (a) Survey of a whole cross-sectioned cell. Bar, 2 μm; (b) Cytoplasmic layer enlarged from a. It contains predominantly a fine filamentous material, which is denser near the cell body. At the periphery of the cell body facing the medium a cortical filamentous network can be detected (indicated by parallel lines), which does not occur in the region of adhesion. Bar, 0.2 μm.

unique opportunity for the description of morphological parameters of cell adhesion in culture as well as for the detection of cytoplasmic contraction and the process of cell movement.

A great many of these observations were made in Dr. E. Kohen's laboratory at the Papanicolaou Cancer Research Institute. It was there that the main theoretical evaluations ripened. We thank Dr. Kohen for his encouraging support and Prof. Grantzer, Frankfurt, for the opportunity to use his microdensitometer, Mrs. M. Vöth for technical assistance in electron microscopy and Mrs. Ingeborg May for photographic assistance, Med. Kand.

REFERENCES

1. ABERCROMBIE, M., and G. A. DUNN. 1975. Adhesion of fibroblasts to substratum during contact inhibition observed by interference reflection microscopy. Exp. Cell Res. 92:57.
2. ALLEN, R. D., and R. R. COWDEN. 1962. Syneresis in ameboid move-

ment: its localisation by interference microscopy and its significance. *J. Cell Biol.* **12**:185.

3. AMBROSE, E. J., and P. C. JONES. 1961. Surface contact microscopy studies in cell movements. *Med. Biol. Illus.* **11**:104.

4. BECK, R., H. HINSSEN, H. KOMNICK, W. STOCKEM, and K. E. WOHL-FARTH-BOTTERMANN. 1970. Weitreichende, fibrilläre Protoplasma-differenzierungen und ihre Bedeutung für die Protoplasma-strömung. V. Kontraktion, ATPase-Aktivität und Feinstruktur isolierter Actomyosin-Fäden von Physarum polycephalum. *Cytobiologie.* **2**:259.

5. BEREITER-HAHN, J. 1971. Möglichkeiten und Grenzen der Auswertung interferenzmikroskopischer Filmaufnahmen lebender Zellen. *Res. Film.* **7**:302.

6. BEREITER-HAHN, J., and L. ELSNER. 1976. Oberflächendifferenzierungen der Fischhaut: zur funktionellen Anatomie der Flammenzellen bei Seepferdchen. Hippocampus kuda Bleeker, Syngnathidae. 9. Koll. d. Arbeitskreises Bedo, Mainz.

7. BEREITER-HAHN, J. 1978. A model for microtubular rigidity. *Cytobiologie.* **17**:298.

8. BIKLE, D., L. G. TILNEY, and K. R. PORTER. 1966. Microtubules and pigment migration in the melanophores of Fundulus heteroclitus L. *Protoplasma.* **61**:322.

9. CURTIS, A. S. G. 1964. The mechanism of adhesion of cells to glass. *J. Cell Biol.* **20**:199.

10. DVORAK, J. A. 1977. Host-parasite relationships at the cellular level in Trypanosoma cruzi infections. *Chagas' Disease Symp. Proc.* 1–10.

11. FORER, A., and R. D. GOLDMAN. 1972. The concentrations of dry matter in mitotic apparatuses in vivo and after isolation from sea-urchin zygotes. *J. Cell Sci.* **10**:387.

12. FRIEND, CH., W. SCHER, J. G. HOLLAND, and T. SATO. 1971. Hemoglobin synthesis in murine virus-induced leukemic cells in vitro: Stimulation of erythroid differentiation by dimethyl sulfoxide. *Proc. Natl. Acad. Sci. U. S. A.* **68**:378.

13. GOLDMAN, R. D., G. BERG, A. BUSHNELL, C.-M. CHANG, L. DICKERMAN, and N. HOPKINS. 1973. Fibrillar systems in cell motility. *Ciba Found. Symp.* **14**:83–107.

14. GOLDMAN, R. D., and D. M. KNIPE. 1973. Functions of cytoplasmic fibers in nonmuscle cell motility. *Cold Spring Harbor Symp. Quant. Biol.* **37**:523–34.

15. GOLDMAN, R. D. 1971. The role of three cytoplasmic fibers in BHK-21 cell motility. I. Microtubules and the effects of colchicine. *J. Cell Biol.* **51**:752.

16. HALE, A. J. 1958. The interference microscope in biological research. Livingstone Ltd., Edinburgh. 114.

17. HEATH, V. P., and G. A. DUNN. 1978. Cell to substratum contacts of chick fibroblasts and their relation to the microfilament system. A correlated interference-reflexion and high voltage electron microscope

study. *J. Cell Sci.* **29**:197.

18. INGRAM, V. M. 1969. A side view of moving fibroblasts. *Nature (Lond.).* **222**:641.

19. IZZARD, C. S., and L. R. LOCHNER. 1976. Cell-to-substrate contacts in living fibroblasts: an interference reflexion study with an evaluation of the technique. *J. Cell Sci.* **21**:129.

20. LAZARIDES, E., and K. WEBER. 1974. Actin antibody: the specific visualization of actin filaments in non-muscle cells. *Proc. Natl. Acad. Sci. U. S. A.* **71**:2268.

21. LOCHNER, L., and C. S. IZZARD. 1973. Dynamic aspects of cell-substrate contact in fibroblast motility. *J. Cell Biol.* **59**:199.

22. LUDUENA, A., and N. K. WESSELLS. 1973. Cell locomotion, nerve elongation, and microfilaments. *Dev. Biol.* **30**:427.

23. MICHEL, K. 1950. Die Grundlagen der Theorie des Mikroskops. Wissenschftl. Verlagsanst., Stuttgard. 314.

24. MITCHISON, J. M., and M. M. SWANN. 1953. Measurements on sea-urchin eggs with an interference microscope. *Quart. J. Microsc. Sci.* **94**:381.

25. OSBORN, M., W. W. FRANKE, and K. WEBER. 1977. Visualization of a system of filaments 7–10 nm thick in cultured cells of an epithelioid line (Pt K2) by immunofluorescence microscopy. *Proc. Natl. Acad. Sci. U. S. A.* **74**:2490.

26. PLOEM, J. S. 1975. Reflection-contrast microscopy as a tool for investigation of the attachment of living cells to a glass surface. *In* Mononuclear Phagocytes in Immunity, Infection and Pathology. R. von Furth, editor. Blackwell Scientific Publications, Melbourne, London. 405–421.

27. POLLARD, TH.D. 1975. Functional implications of the biochemical and structural properties of cytoplasmic contractile proteins. *In:* Molecules and Cell Movement. (S. Inoué et al., editors. Raven Press, N. Y. 259–286.

28. REES, D. A., C. W. LLOYD, and D. THOM. 1977. Control of grip and stick in cell adhesion through lateral relationships of membrane glycoproteins. *Nature (Lond.).* **267**:124.

29. REVEL, J. P., and K. WOLKEN. 1973. Electron microscope investigations of the underside of cells in culture. *Exp. Cell Res.* **78**:1.

30. THORELL, B. 1947. Studies on the formation of cellular substance during blood cell production. Diss. Karolinska Inst., Stockholm.

31. TILNEY, L. G. 1975. The role of actin in non-muscle cell motility. *In* Molecules and Cell Movement. S. Inoué et al., editors. Raven Press, N. Y. 339–388.

32. WEBER, K., R. POLLACK, and TH. BIBRING. 1975. Antibody against tubulin: the specific visualization of cytoplasmic microtubules in tissue culture cells. *Proc. Natl. Acad. Sci. U. S. A.* **72**:459.

33. WESSELLS, N. K., B. S. SPOONER, and M. A. LUDUENA. 1973. Surface movements, microfilaments and cell locomotion. *Ciba Found. Symp. Quant. Biol.* **14**:53–82.